ELSEVIER

Journal of Alloys and Compounds 217 (1995) 13–21

Journal of ALLOYS AND COMPOUNDS

Solid state phase equilibria in the Ni–Al–As system

S. Députier[a], R. Guérin[a,*], Y. Ballini[b], A. Guivarc'h[b]

[a]Laboratoire de Chimie du Solide et Inorganique Moléculaire, UA CNRS 1495, Université de Rennes I, Avenue du Général Leclerc, F-35042 Rennes Cedex, France

[b]FRANCE TELECOM, Centre National d'Etudes des Télécommunications, Lannion B, BP 40, F-22301 Lannion Cedex, France

Received 18 March 1994

Abstract

Solid state phase equilibria in the ternary Ni–Al–As diagram were established at 800 °C. The experimental techniques used to elaborate the phase equilibria were X-ray diffraction (XRD), electron probe microanalysis (EPMA) and scanning electron microscopy (SEM). Three ternary phases, which crystallize in hexagonal symmetry and are all structurally derived from the NiAs type, were evidenced in the Ni-rich part of the diagram. Among them, two ternaries labelled as A and D phases, by comparison with the isostructural ternary phases in the Ni–Ga–As diagram, reveal fully disordered structures; in contrast, the ternary B phase shows a hexagonal superlattice ($a\sqrt{3}$, $3c$), which denotes an ordered structure. Very limited solid solubilities were measured in the binary constituent Ni–Al and Ni–As compounds, with the exception of NiAs which showed a homogeneity range with an Al-rich limit corresponding to the formula $NiAs_{0.7}Al_{0.3}$. Neither nickel nor ternary phases are in thermodynamic equilibrium with AlAs, in contrast with the binaries NiAl, Ni_2Al_3 and NiAs which are. The bottom part of the experimental diagram differs from the theoretical one deduced from estimated thermodynamic data on Ni–Al and Ni–As binaries using Miedema's model, but is in agreement with interfacial reaction studies which concluded that NiAl and substituted NiAs are the stable phases when Ni thin films are reacted to completion on AlAs. Finally, the influence of the IIIa element (Ga or Al) in the Ni–IIIa–As systems was considered through a comparative study between Ni–Ga–As and Ni–Al–As diagrams. The pseudoternary Ni–(Ga,Al)–As system was experimentally estimated for the atomic composition ($Ga_{0.7}Al_{0.3}$), which is the value usually chosen for the elaboration of GaAs/(Ga,Al)As heterostructures with $Ga_{1-x}Al_xAs$ exhibiting a direct gap of highest energy.

Keywords: Solid state phase equilibria; X-ray diffraction; Electron probe microanalysis; Scanning electron microscopy

1. Introduction

The advent of III–V integrated circuits, their miniaturization and their integration requires the development of rectifying and low resistance contacts which are adherent, reproducible, stable and laterally uniform. During the past decade a large number of studies of the chemistry at metal/III–V compound semiconductor interfaces (M/III–V) have been published which concluded the importance of phase diagrams. Indeed, the M–III–V ternary diagram provides a useful framework for rationalizing the reactions of metals with III–V semiconductors and for researching stable metallization materials. Our own studies on Ni/GaAs, Rh/GaAs and Er/GaAs contacts [1–4] together with those on Rh_2As/GaAs, RhGa/GaAs, Ni_2Ga_3/GaAs, NiGa/GaAs and ErAs/GaAs heterostructures [5–9], based on knowledge of the experimental ternary diagrams Ni–Ga–As, Rh–Ga–As and Er–Ga–As [1,10,11], led to a general approach for metallization contacts consisting of three successive steps: firstly, the experimental determination of the ternary M–III–V phase diagram; secondly, the study of the solid state interdiffusions M/III–V; finally, the codeposition of stable and epitaxial M_xIII_y, M_xV_y or $M_xIII_yV_z$ metallic compounds in a molecular beam epitaxy (MBE) system.

Within this context we conjointly studied the ternary Ni–Al–As phase diagram and the solid state interdiffusions between Ni thin films and AlAs substrates. The choice of the Ni/AlAs contact results on one hand from the absence of any information about mutual interactions between the three elements Ni, Al and As and on the other hand from the analogy between Ni–Ga and Ni–Al binary systems. Indeed, the recent interest

*Corresponding author.

SSDI 0925-8388(94)01296-T

in epitaxial NiGa and Ni_2Ga_3 contacts on GaAs [7] has enabled one to predict the elaboration of NiAl or Ni_2Al_3/AlAs (or /GaAs or /(Ga,Al)As) heterostructures. These heterostructures should be more stable in temperature than those with NiGa and Ni_2Ga_3 owing to the increase in thermal stability of NiAl (T_f = 1638 °C) and Ni_2Al_3 (T_f = 1133 °C) compared with that of the isostructural binaries NiGa (T_f = 1220 °C) and Ni_2Ga_3 (T_f = 895 °C).

This paper first reports on the isothermal section of the bulk Ni–Al–As phase diagram determined experimentally at 800 °C. Then a comparative study with the ternary phase diagram calculated from estimated thermodynamic data on the binary compounds using Miedema's model has been made in order to test the validity of the calculated diagram. Finally, the isothermal section of the Ni–Al–As phase diagram has been compared with the Ni–Ga–As one that we previously elaborated. The Ni–(Ga,Al)–As pseudoternary system has been studied for the atomic composition ($Ga_{0.7}Al_{0.3}$), which is the value usually chosen for the elaboration of GaAs/(Ga,Al)As heterostructures, since this Al concentration allows one to increase the gap and to maintain it direct. The results on the interfacial reactions of Ni thin films on (001) and (111) AlAs, which are in agreement with the experimental bulk phase diagram, will be published elsewhere [12].

2. Experimental determination of the Ni–Al–As phase diagram

2.1. Experimental details

The binary Ni_xAl_y compounds were previously prepared by combining the required amounts of the elements; the starting materials were either powders (nickel and aluminium) or ingots (aluminium), all with minimum purity 99.9%. All samples (about 800 mg each) were melted (after cold pressing as pellets if necessary) in an arc furnace using a non-consumable thoriated tungsten electrode in a Ti/Zr-gettered argon atmosphere. In order to ensure homogeneity, the samples were turned and remelted several times. Weight losses due to the arc-melting process were found to be insignificant (less than 1 wt.%).

The ternary $Ni_xAl_yAs_z$ compounds were synthesized at a temperature of 800 °C by combining either the Ni_xAl_y alloys with amorphous β-As powder or the three elements as powders. Since elemental aluminium reacts strongly with silica above 700 °C, samples were cold pressed and placed in boron nitride crucibles within quartz ampoules which were evacuated to about 10^{-3} Torr, sealed and placed in a resistance furnace. They were first annealed at 800 °C for 72 h, cooled, ground to powder, cold pressed into pellets, sealed again and annealed for 20 days to ensure homogeneity. Finally, samples were quenched in ice water. In fact, numerous grindings and re-annealings at the same temperature for a long time were needed to reach thermodynamic equilibrium.

At the end, the pellets were removed from the quartz ampoules and cut in half. One half of each sample was pulverized and analysed using a powder diffractometer (CPS 120 INEL) equipped with a position-sensitive detector covering 120° in 2θ (elemental silicon was taken to determine a cubic spline calibration function to describe the 2θ vs. channel number function). The second half was embedded in epoxy resin and polished down to 0.25 mm diamond grade. The sample was then coated with either a gold or graphite thin layer to obtain a good surface conductivity. Composition analysis was done with a Camebax SX 50 electron microprobe using wavelength-dispersive spectroscopy (WDS) of X-rays. Al_2O_3, NiO and AlAs were used as standards. Backscatterd electron imaging was done with a Jeol JSM-35C scanning electron microscope. The compositional data were carefully checked against the diffraction data to identify the phases present in each sample.

2.2. The constituent binaries

Prior to discussing the experimental data obtained in the present study for the Ni–Al–As ternary system at 800 °C, let us first review the binary data reported in the literature [13–25]. The phase stabilities and crystallographic data of intermediate binary phases are best known as the Al–As and Ni–As systems, followed by the Ni–Al one. The X-ray diffraction patterns of the binaries observed in this study at 800 °C were compared with those previously reported.

The only intermediate phase in the Al–As system is AlAs; its structure, lattice parameter and melting point taken from the literature are given in Table 1.

Four intermediate phases occur in the Ni–As system: Ni_5As_2, $Ni_{11}As_8$, NiAs and $NiAs_2$. Among them, $NiAs_2$ exhibits two allotropic modifications: α-$NiAs_2$ (orthorhombic *Pbca*) for $T < 590$ °C and β-$NiAs_2$ (orthorhombic *Pnnm*) for $T > 590$ °C. The structural data and temperature stabilities for all the binaries in the Ni–As system are summarized in Table 1.

Previous investigations [20–25] and our own studies have revealed that several intermediate phases occur in the Ni–Al system: Ni_3Al, Ni_2Al, Ni_5Al_3, NiAl, Ni_3Al_4, Ni_2Al_3 and $NiAl_3$. Among them, Ni_2Al, Ni_5Al_3 and Ni_3Al_4 have not been observed at 800 °C; indeed, Ni_3Al_4 decomposes at 580 °C ($Ni_2Al_3 + NiAl \leftrightarrow Ni_3Al_4$) and Ni_5Al_3 at 700 °C ($Ni_3Al + NiAl \leftrightarrow Ni_5Al_3$). Finally, numerous re-annealings at about 300–400 °C for a long time are needed to obtain Ni_2Al, which has been reported as being structurally a superstructure of Ni_5Al_3

Table 1
Ni–Al–As constituent binary phases, crystal structures, lattice parameters and temperature stabilities

Phase	Structure type, Pearson symbol	Lattice parameters (nm)	Temperature stability (°C)[a]	Refs.
Ni_5As_2	Ni_5As_2, hP42	$a=0.6799(2)$; $c=1.12456(4)$	998 (c)	[13,16]
$Ni_{11}As_8$	$Ni_{11}As_8$, tP76	$a=0.6852(7)$, $c=2.181(3)$	830 (p)	[13,15]
NiAs	NiAs, hP4	$a=0.3618(2)$, $c=0.5034(3)$	962 (c)	[13,17]
$NiAs_2$ (α)	$NiAs_2$, oP24	$a=0.57718(5)$, $b=0.58342(6)$, $c=1.14214(12)$	<600	[13,18]
$NiAs_2$ (β)	FeS_2 (m), oP6	$a=0.4757(7)$, $b=0.5803(8)$, $c=0.3556(8)$	600–1040 (c)	[13,19]
Ni_3Al	Cu_3Au, cP4	$a=0.35635(5)$ $a=0.35610(9)$[b]	1395 (p)	[13,20]
Ni_2Al	Ni_2Al_3, hP5	$a=0.40828$, $c=0.50004$		[13,21]
Ni_5Al_3	"Pt_5Ga_3", oC16	$a=0.7475$, $b=0.6727$, $c=0.3732$	700 (pd)	[13,14]
NiAl	CsCl, cP2	$a=0.2848(14)$ $c=0.28874(6)$[b]	1638 (c)	[13,14]
Ni_3Al_4	Ni_3Ga_4, CI112	$a=1.1408(1)$	580 (pd)	[13,23]
Ni_2Al_3	Ni_2Al_3, hP5	$a=0.40339$, $c=0.48938$ $a=0.4037(1)$[b], $c=0.4899(2)$[b]	1133 (p)	[13,24]
$NiAl_3$	Fe_3C, oP16	$a=0.6598$, $b=0.7352$, $c=0.4802$ $a=0.6609(2)$[b], $b=0.7356(1)$[b], $c=0.4804(2)$[b]	854 (p)	[13,14]
AlAs	ZnS, cF8	$a=0.56610$	1760 (c)	[13,14,25]
Ni	Cu, cF4	$a=0.35236$	1455	[13,14]
Al	Cu, cF4	$a=0.404950(12)$	660	[13,14]
As	α-As, hR2	$a=0.37598(1)$, $c=1.05475(2)$	614	[13,14]

[a]Key: c, congruent melting, p, peritectic melting; pd, peritectoid decomposition.
[b]Unit cell parameters which have been refined in this work.

[21]. With the exception of $NiAl_3$, the binaries Ni_3Al, NiAl and Ni_2Al_3 show homogeneity ranges at 800 °C, especially the last two. In our experiments, NiAl extends from 46 to 60 at.% Ni instead of from 44 to 62 at.% Ni as given in the literature. The cubic unit cell constant first increases from $a=0.2866(1)$ nm for $Ni_{46}Al_{54}$ to $a=0.2892(1)$ nm for $Ni_{50}Al_{50}$ (filling up of constitutional defects in the Ni sublattice) and then decreases to $a=0.2867(1)$ nm for $Ni_{60}Al_{40}$ (excess Ni atoms substituting in the Al sublattice) [26]. The homogeneity range that we found for Ni_2Al_3 extends from 39 to 44 at.% Ni instead of from 38 to 43 at.% Ni as given in the literature. The solubility maximum of Al in (Ni) is about 10% at 800 °C.

2.3. The ternary Ni–Al–As system

2.3.1. The general features

According to the review given above, the stable binary phases at 800 °C are Ni_3Al, NiAl, Ni_2Al_3, $NiAl_3$, Ni_5As_2, $Ni_{11}As_8$, NiAs, $NiAs_2$ and AlAs. On the basis of these binaries, the Ni–Al–As phase diagram has been built (pure aluminium is the only liquid phase at the diagram temperature). The general rules to elaborate such ternary diagrams have been the subject of previous papers [10,27,28]. A total of about 50 samples were prepared to establish the solid state phase equilibria of the Ni–Al–As system at 800 °C (Fig. 1). The gross compositions of some samples (labelled 1–15], the phases identified by X-ray diffraction (XRD) and the compositions of the phases as determined by electron probe microanalysis (EPMA) are listed in Table 2.

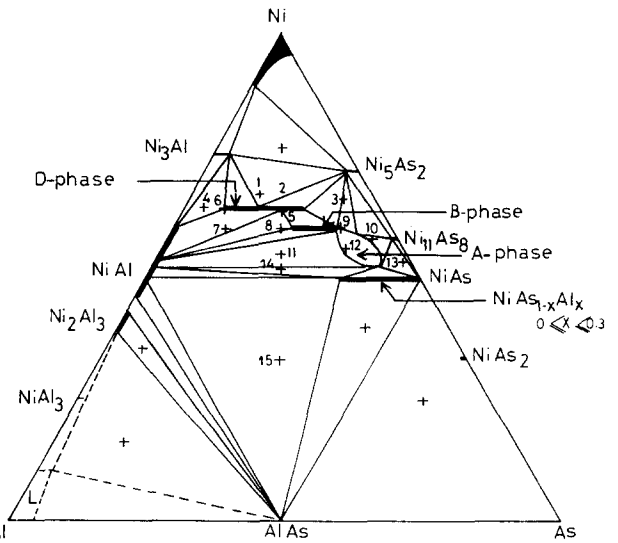

Fig. 1. Isothermal section of Ni–Al–As ternary diagram at 800 °C. Axes are in at.%. Compositions of samples 1–15 reported in Table 2 are indicated.

Most of the binary phases in the system reveal small ternary solubilities, with the exception of NiAs which dissolves about 15 at.% Al leading to the Al-rich limit $NiAs_{0.7}Al_{0.3}$. The small solubilities in the other binaries were mainly established on the basis of EPMA of equilibrated heterogeneous samples of overall compositions as indicated in Fig. 1 and Table 2.

The main feature of this isothermal section is the existence of several ternary phases with extended homogeneity ranges in the Ni-rich part of the diagram. XRD studies have shown that all these phases are similar to those reported in the Ni–Ga–As system. This result is not surprising, since the covalent radii of Ga and Al are both equal to 0.126 nm [29]. Therefore the nature of the phases and their composition must be very close to each other in the two systems; indeed, all the phases found in the Ni–Ga–As and Ni–Al–As phase diagrams are derivative from the NiAs type and exhibit either ordered or fully disordered structures.

Table 2
Gross sample compositions and phases identified by X-ray diffraction and EPMA for 800 °C isotherm

Sample number	Gross composition (at.%)			Phases identified by X-ray diffraction	Composition of phases by EPMA (at.%)		
	Ni	Al	As		Ni	Al	As
1	65	21	14	D phase	66.6	19.7	13.6
				Ni_5As_2	69.6	1.1	29.2
				Ni_3Al	74.5	22.6	2.9
2	65	16	19	D phase	66.4	20	13.6
				Ni_5As_2	70.1	0.7	29.2
3	65	5	30	B phase	60.5	8.1	31.4
				Ni_5As_2	69.7	0.4	29.9
4	64	32	4	D phase	66.1	24	9.9
				NiAl	60.5	39.1	0.4
				Ni_3Al	73.1	23.6	3.3
5	63.6	18.2	18.2	D phase	64.3	18.9	16.8
6	63.6	27.3	9	D phase	64.3	19.4	16.3
				NiAl	57.6	42.2	0.2
7	60	30	10	D phase	65.1	20	14.9
				NiAl	53	47	0
8	60	20	20	B phase	61.6	12.1	26.3
				NiAl	55.7	44.2	0.1
9	60	10	30	B phase	59.8	9.2	31
10	58	5	37	$Ni_{11}As_8$	56.7	0.3	42.9
				A phase	59.4	6.1	34.4
11	55.5	22.2	22.2	A phase	58	8	34.0
				NiAl	53.1	46.8	0.1
12	55.5	11.1	33.3	A phase	58	8.9	33.1
13	54	2	44	NiAs	49.6	0	50.4
				$Ni_{11}As_8$	56.8	0	43.2
14	52.4	23.8	23.8	A phase	54	6.6	39.4
				NiAl	51.5	48.4	0.1
15	33.3	33.3	33.3	NiAl	54.3	45.7	0.1
				NiAs	49.4	15.5	35
				AlAs	–	–	–

Although five phases were found in the Ni–Ga–As system, only three phases labelled A, B and D, by comparison with the isostructural Ga-based ternaries, have been observed in the Ni–Al–As one. These phases exhibit broad homogeneity ranges and are slightly shifted towards an As-rich atomic composition with respect to the corresponding Ga-based phases. The A, B and D phases, which show either disordered or ordered structures derivative from the NiAs type (see below), are displayed along the NiAs–$Ni_{3.5}$AlAs composition line. The miscibility gaps which occur along this line seem to correspond in fact to a sequence of successively disordered and ordered crystal structures.

In contrast, the phases labelled C and E in the Ni–Ga–As phase diagram were not found here in the Ni–Al–As one. In fact, the composition of the E phase is included in the homogeneity range of the A phase, while the C phase, which was considered as being a substituted Ga–As solid solution derivative from the binary Ni_3Ga_2 [10], cannot exist in the Ni–Al–As diagram, since the corresponding Al-based binary belongs here to the NiAl solid solution.

Finally, it is worth noticing that the occurrence in the Ni-rich part of the diagram of three ternary phases with extended homogeneity ranges and structurally related to each other made difficult the determination of the composition ranges and the setting of the tie-lines which delimit two-phase and subsequently three-phase regions. Moreover, the homogeneity range of the binary NiAl is important and NiAs generates a substituted solid solution. The more probable tie-lines and composition limits in the upper part of the phase diagram, deduced from the electron probe microanalyses conjointly with the XRD experiments, are shown in Fig. 1 and Table 2. For example, a scanning electron backscatter micrograph of sample 2 which displays a two-phase region consisting of Ni_5As_2 (smaller granular areas) and D phase (large plates) is presented in Fig. 2a, while a micrograph of sample 15 exhibiting the microstructure of an NiAl and NiAs mixture is shown in Fig. 2b.

Another important result is the fact that a three-phase region consisting of AlAs, NiAl and NiAs dominates the AlAs side of the ternary Ni–Al–As phase diagram; neither $NiAs_2$ nor $NiAl_3$ has been found in thermodynamic equilibrium with AlAs at 800 °C, in contrast with NiAs, NiAl as well as Ni_2Al_3 which are. The last result is of importance for the fabrication of stable AlAs/NiAl/AlAs and AlAs/Ni_2Al_3/AlAs heterostructures (also with GaAs or (Ga,Al)As substrates).

In the classification of ternary phase diagrams described by Beyers et al. [28], the Ni–Al–As system could

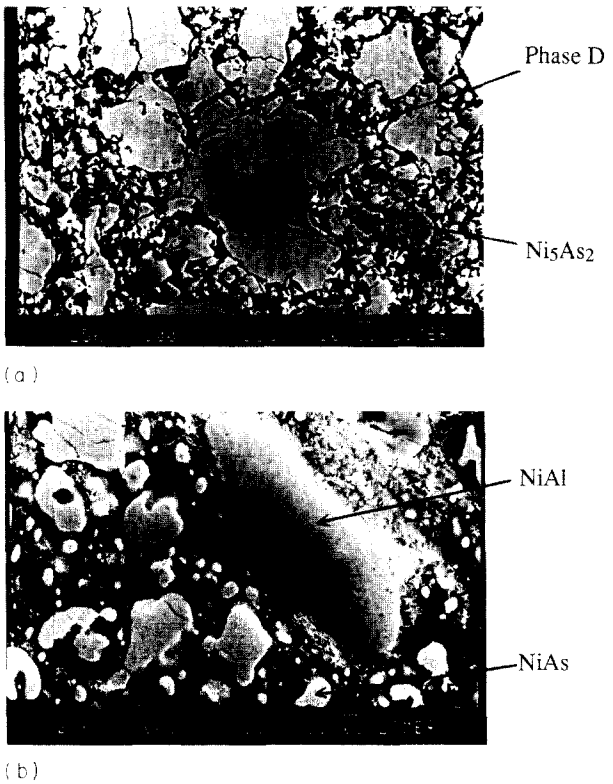

Fig. 2. Scanning electron backscatter micrographs showing phase mixtures: a, D phase and Ni_5As_2 (sample 2); b, NiAl and NiAs (sample 15).

be seen as belonging to type V, since ternary phases exist. Nevertheless, these phases are not in thermodynamic equilibrium with AlAs; therefore all the general features of the diagram correspond essentially to type IV.

2.3.2. The ternary phases

The three phases A, B and D observed in the Ni–Al–As diagram crystallize in hexagonal symmetry and exhibit crystal structures which are derivative from the NiAs-type structure ($B8_1$) (Fig. 3). This latter structure, with two formula units per cell, shows the metal and non-metal atoms occupying the 2*a* (0 0 0, 0 0 $\frac{1}{2}$) and 2*c* ($\frac{1}{3}$ $\frac{2}{3}$ $\frac{1}{4}$, $\frac{2}{3}$ $\frac{1}{3}$ $\frac{3}{4}$) positions of the space group $P6_3/mmc$ respectively. Moreover, two additional sites 2*d* ($\frac{1}{3}$ $\frac{2}{3}$ $\frac{3}{4}$, $\frac{2}{3}$ $\frac{1}{3}$ $\frac{1}{4}$) are vacant which can be fully or partly occupied by metal atoms. When these sites are fully occupied, one obtains the Ni_2In-type structure ($B8_2$) which is called the "filled-up" NiAs-type structure [30]. When both sites are half occupied, the obtained structure is that of the binary Ni_3Ga_2 ($8_{1.5}$) in its high temperature modification γ, for which no superstructure is reported [31].

By considering the covalent radii of arsenic and aluminium as 0.118 and 0.126 nm respectively [28], one can predict that the substitution of arsenic by aluminium atoms in the NiAs structure would expand the non-metal sublattice and therefore would increase the nickel

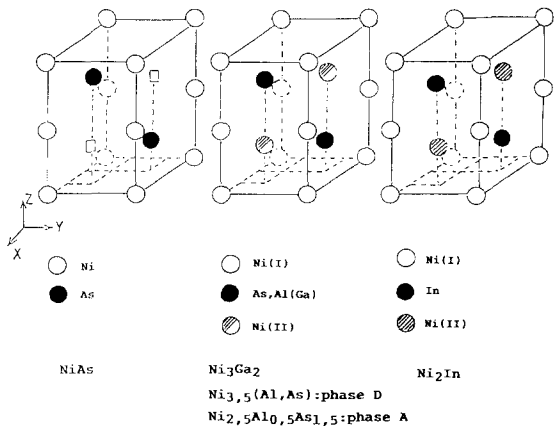

Fig. 3. Representation of structures NiAs ($B8_1$), $Ni_{3.5}AlAs$ ($B8_{1.5}$) and Ni_2In ($B8_2$). Ni and non-metal atoms are denoted by white and black circles respectively; extra Ni atoms in half- (e.g. $Ni_{3.5}AlAs$) or full (Ni_2In) occupancy are represented by streaked circles.

content; this assumption has been effectively checked. The Ni insertion and the As–Al substitution obey to two different structural mechanisms.

(1) If no crystallographic ordering governs both the As–Al substitution in the non-metal sublattice and the Ni insertion, the structure will obviously be disordered and will remain of NiAs type with lattice constants (*a*, *c*) of the same order of magnitude.

(2) If a crystallographic ordering occurs either on the non-metal sublattice or in the distribution of additional nickel atoms, it will necessarily induce superstructures derivative from the NiAs-type structure, thus giving extra reflections in the XRD powder pattern.

The crystallographic data of the three ternary phases in the Ni–Al–As diagram show that they correspond to either one or other of these structural mechanisms. These phases are now discussed.

A phase. This phase is the major solid phase of the Ni–Al–As diagram. In comparison with that of the Ni–Ga–As diagram, the A phase is shifted slightly towards arsenic-rich compositions, since it extends approximately over the range of atomic compositions from $Ni_xAl_{0.6}As_{1.4}$ (Al-rich limit) to $Ni_xAl_{0.35}As_{1.65}$ (As-rich limit) with x varying between 2.2 to 3. The atomic composition of the E phase (i.e. $Ni_{2.33}Ga_{0.35}As_{1.65}$ in the Ni–Ga–As diagram) [10] belongs now to the homogeneity range of the A phase. Since no extra reflections have been observed in the XRD powder pattern (Fig. 4, top), the crystal structure of the A phase can be considered as being wholly disordered of NiAs type. The structure determination of the corresponding Ga-based phase that we previously solved confirmed this assumption [10]. Crystallographic data for several compositions of the A phase are given in Table 3.

B phase. The As-rich part of this phase borders the previous one and shows a somewhat narrow homogeneity range with an unvarying nickel content of 60 at.%. The B phase extends from the atomic composition

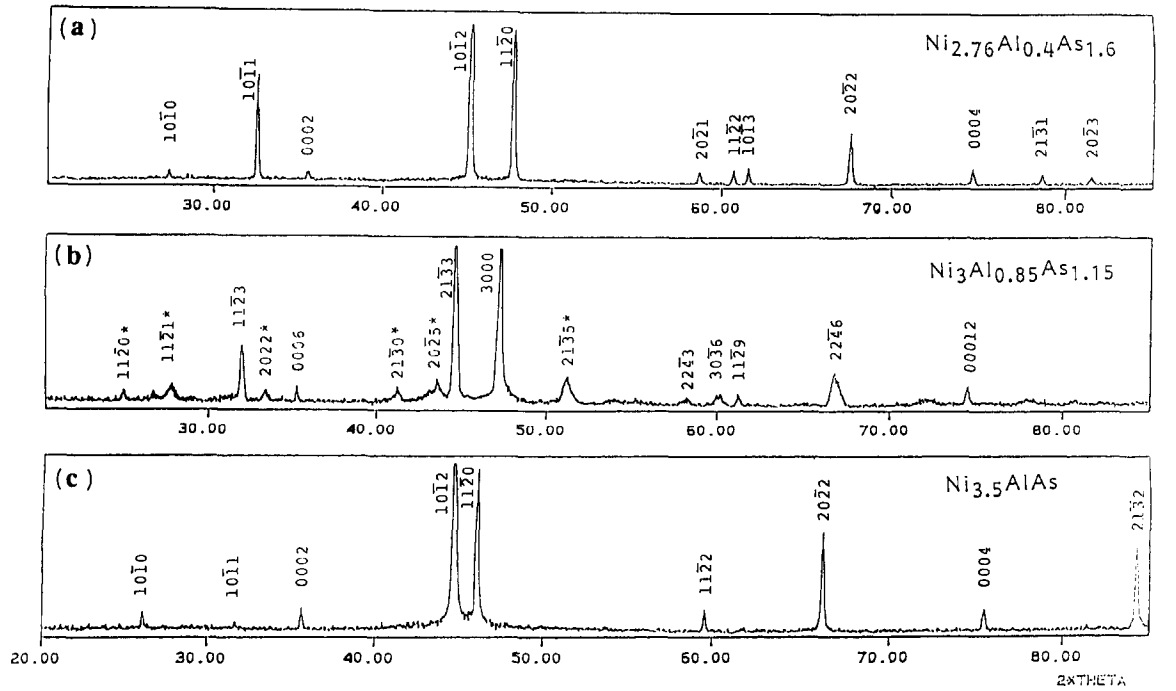

Fig. 4. X-Ray diffraction patterns for ternary compositions $Ni_{2.76}Al_{0.4}As_{1.6}$ (A phase), $Ni_3Al_{0.85}As_{1.15}$ (B phase) and $Ni_{3.5}AlAs$ (D phase) ($\lambda_{Cu}=0.154056$ nm).

Table 3
Crystallographic data for various atomic compositions of ternary A, B and D phases and pseudobinary NiAs phase

Composition (at.%)	Formula	*a* (nm)	*c* (nm)	*V* (10^{-3} nm^3)	*c/a*
A phase					
$Ni_{60}Al_8As_{32}$	$Ni_3Al_{0.4}As_{1.6}$	0.3836 (1)	0.5115 (2)	65.18	1.334
$Ni_{58}Al_8As_{34}$	$Ni_{2.76}Al_{0.4}As_{1.6}$	0.3816 (1)	0.5096 (3)	64.26	1.335
$Ni_{56}Al_{13}As_{31}$	$Ni_{2.5}Al_{0.6}As_{1.4}$	0.3779 (1)	0.5061 (1)	62.59	1.339
$Ni_{54}Al_8As_{38}$	$Ni_{2.35}Al_{0.35}As_{1.65}$	0.3685 (1)	0.5035 (3)	59.23	1.366
B phase					
$Ni_{60}Al_{17}As_{23}$	$Ni_3Al_{0.85}As_{1.15}$	0.6687→0.3861 (4)[a]	1.5318→0.5106 (7)[a]	593.2→65.92[a]	2.291→1.322[a]
$Ni_{60}Al_{10}As_{30}$	$Ni_3Al_{0.5}As_{1.5}$	0.6661→0.3846 (2)[a]	1.5321→0.5107 (4)[a]	588.7→65.42[a]	2.300→1.328[a]
D phase					
$Ni_{64}Al_{15}As_{22}$	$Ni_{3.5}Al_{0.8}As_{1.2}$	0.3937 (2)	0.5089 (5)	68.31	1.293
$Ni_{64}Al_{18}As_{18}$	$Ni_{3.5}AlAs$	0.3959 (2)	0.5064 (7)	68.74	1.279
$Ni_{64}Al_{20}As_{16}$	$Ni_{3.5}Al_{1.1}As_{0.9}$	0.3968 (1)	0.5039 (2)	68.71	1.270
$Ni_{64}Al_{27}As_9$	$Ni_{3.5}Al_{1.5}As_{0.5}$	0.3973 (1)	0.5027 (2)	68.72	1.265
Pseudobinary NiAs phase					
$Ni_{50}As_{50}$	NiAs	0.3613 (1)	0.5024 (2)	56.79	1.390
$Ni_{50}Al_{10}As_{40}$	$Ni_2Al_{0.4}As_{1.6}$	0.3627 (1)	0.5030 (2)	57.31	1.387
$Ni_{50}Al_{15}As_{35}$	$Ni_2Al_{0.6}As_{1.4}$	0.3654 (2)	0.5031 (3)	58.20	1.377

[a]Data for NiAs subcell.

$Ni_3Al_{0.85}As_{1.15}$(Al-rich limit) to $Ni_3Al_{0.5}As_{1.5}$ (As-rich limit). By comparison with the corresponding Ga-based phase, the XRD powder pattern of this phase has been indexed in a hexagonal superlattice with the constants $a\sqrt{3}$ and 3*c*. This ordered structure, derivative from the NiAs type, explains the occurrence of extra reflections in the XRD powder data (Fig. 4, middle). Electron diffraction patterns taken during transmission electron microscopy (TEM) studies on Ni/AlAs (111) samples after annealing at 250 °C have recently confirmed the existence of the $a\sqrt{3}$, 3*c* superlattice of the B phase [32]. Since the atomic Al/As ratio varies in the overall composition range of the B phase without modification of the Ni content, it can be concluded that the structure ordering is due to the filling of one of the two vacant 2*d* sites by the additional Ni atom in the NiAs-type

Table 4
Calculated formation enthalpies of Ni–Al and Ni–As binaries

Compound	$NiAl_3$	Ni_2Al_3	NiAl	Ni_3Al	Ni_5As_2	$Ni_{11}As_8$	NiAs	$NiAs_2$	AlAs[a]
$-\Delta H_0$ (kJ mol^{-1})	28.2	42.9	47.7	33.0	40.2	47.9	46.8	34.6	60.4

[a]Experimental value.

structure. Crystallographic data for two atomic compositions of the B phase are presented in Table 3.

D phase. This phase shows a wide homogeneity range owing to the Al–As substitution without any apparent modifications of the nickel content (64 at.%). The atomic Al-rich composition is $Ni_{3.5}Al_{1.5}As_{0.5}$, while the As-rich one corresponds to $Ni_{3.5}Al_{0.8}As_{1.2}$. Without extra lines in the XRD powder pattern (Fig. 4, bottom), one can conclude that the D phase has a wholly disordered structure NiAs type, as has been confirmed by the structure determination of the corresponding Ga-based phase [10]. In addition, it can also be noticed that the D phase contains $Ni_{3.5}AlAs$ in its homogeneity range, which is the only ternary compound to exhibit a stoichiometric content of aluminium and arsenic in the phase diagram. This result is of interest in the case of Ni/AlAs solid state interdiffusions, since the average composition of a reacted Ni thin film remains on the vertical line connecting Ni and AlAs; with the exception of the compound $Ni_{3.5}AlAs$, the other products of the interaction Ni/AlAs will be mixtures of two or three phases. However, $Ni_{3.5}AlAs$ which is not in equilibrium with AlAs could not give a thermodynamically stable contact on the III–V substrate. Crystallographic data for several compositions of the D phase are given in Table 3.

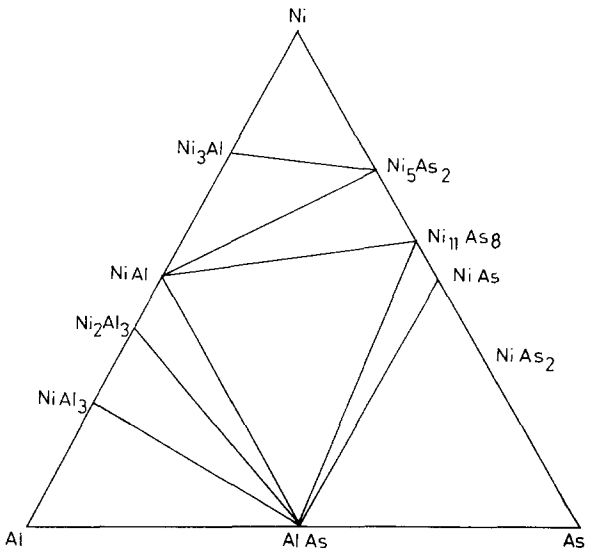

Fig. 5. Ni–Al–As ternary diagram calculated from Miedema's model.

3. The calculated Ni–Al–As phase diagram

The standard enthalpies of formation for the binary systems Ni–Al and Ni–As (Table 4) – calculated by using the "semiempirical" Miedema model [33–36] because of the deficiency of true experimental thermodynamic data – allow us to elaborate a theoretical Ni–Al–As ternary diagram (Fig. 5). This diagram differs significantly from the experimental one, showing in particular a wrong three-phase region NiAl–$Ni_{11}As_8$–AlAs involving an NiAl–$Ni_{11}As_8$ tie-line instead of the true NiAl–NiAs one; in fact, the NiAs–$NiAl_{0.3}As_{0.7}$ solid solution prevents the existence of an AlAs–$Ni_{11}As_8$ tie-line. This is of importance in studies of solid state interdiffusions Ni/AlAs, while the last step of the interaction, when Ni thin films are reacted to completion on AlAs, corresponds to an average atomic composition Ni_xAlAs which is a mixture of two binaries NiAl and NiAs [12]. Moreover, calculations from Miedema's model take no account of the existence of ternary or pseudobinary phases in the upper part of the diagram, which do not permit one to clearly understand the first successive steps of the Ni/AlAs interaction. These results point out the limitations of theoretical calculations based on Miedema's model in determining ternary phase diagrams.

4. The pseudoternary Ni–(Ga,Al)–As phase diagram

The solid portion of the Ni–Ga–As phase diagram at 800 °C is shown in Fig. 6a. As previously mentioned, five ternary phases, A, B, C, D and E, which crystallize in hexagonal symmetry and may be structurally derived from the NiAs type, were evidenced in the upper part of the Ni–Ga–As phase diagram [10]. While the A and D phases were found to be wholly disordered, the B, C and E phases showed hexagonal superlattices, with lattice constants $a\sqrt{3}\times 3c$, $2a\times 4c$ and $3a\times 2c$ respectively. Among these phases, only the A, B and D phases are present in the Ni–Al–As diagram (Fig. 6b). While gallium and aluminium can be considered as being chemically and structurally very close to each other, the absence of the C phase in the Ni–Al–As system induces some modifications between the two phase diagrams, especially in the setting of the tie-lines. Such a result leads to significant differences in the solid state

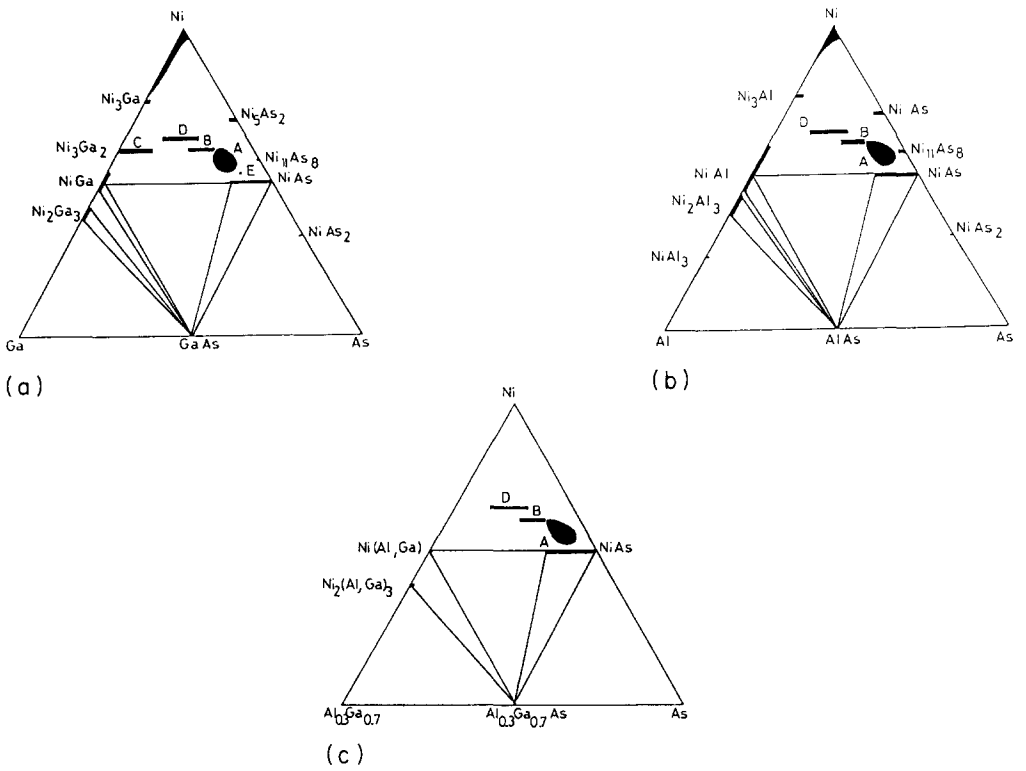

Fig. 6. Isotherm sections at 800 °C of (a) Ni–Ga–As, (b) Ni–Al–As and (c) Ni–$Ga_{0.7}Al_{0.3}$–As (800 °C) phase diagrams. For simplification, only the ternary phases have been located in the Ni-rich part of the diagrams. The tie-lines, which are of great importance for determining potential binary candidates in metallization contacts on III–V semiconductors, are drawn in the bottom part.

interdiffusions Ni/GaAs and Ni/AlAs [2,12]. For example, NiAs appears as the "key" compound around which the Ni/GaAs interaction evolves (mixtures of NiAs with either the A, E or C phase), while NiAl is that of the Ni/AlAs one (mixtures of NiAl with either the D or B phase). Nevertheless, in both cases the last steps are equivalent, leading to mixtures of high textured NiGa or NiAl with pseudocubic grains of substituted NiAs.

The numerous studies on GaAs/(Ga,Al)As heterostructures in order to obtain multiquantum wells induce us to realize Ga–Al substitution attempts within the five ternary phases of the Ni–Ga–As system. For this study, as justified before, we have chosen the atomic Ga/Al ratio as 0.7/0.3. The pseudoternary phases $Ni_{3.5}(Ga_{1-x}Al_x)As$, $Ni_3(Ga_{1-x}Al_x)_{1.75}As_{0.25}$, $Ni_{2.5}(Ga_{1-x}Al_x)_{0.5}As_{1.5}$, $Ni_3(Ga_{1-x}Al_x)_{0.85}As_{1.15}$ and $Ni_{2.33}(Ga_{1-x}Al_x)_{0.35}As_{1.65}$ with $x=0.3$, corresponding to the D, C, A, B and E phases respectively, have been synthesized. Among them, the E phase has not been found, nor the C phase; in the latter case a mixture consisting of the D phase and the $Ni(Ga_{0.7}Al_{0.3})$ pseudobinary was obtained. In contrast, the pseudoternaries corresponding to the A, B and D phases showed XRD powder patterns similar to those of the ternaries. Therefore by extrapolation the Ni–(Ga,Al)–As phase diagram has been built (Fig. 6(c)); this diagram looks like the Ni–Al–As one. It can be concluded that the metallurgy of the $Ni/Ga_{0.7}Al_{0.3}As$ contact should be closer to that of Ni/AlAs than that of the Ni/GaAs one.

5. Conclusions

In this study the isothermal phase diagram for Ni–Al–As was determined at 800 °C. Limited solubility was measured in each of the constituent binary phases, with the exception of NiAs which dissolves 15 at.% Al (nominal composition $NiAs_{0.7}Al_{0.3}$). The existence of three ternary phases with broad homogeneity ranges located in the upper part of the diagram was pointed out. All these phases crystallize in hexagonal symmetry and may be structurally derived from the NiAs type with either disordered or ordered structures. The occurrence of an AlAs–NiAl–NiAs three-phase equilibrium triangle, not suggested by theoretical calculations on the formation enthalpies of Ni–Al, Ni–As and Al–As binaries using Miedema's model, was experimentally evidenced. Finally, a comparative study of the quite equivalent Ni–Ga–As and Ni–Al–As diagrams pointed out some differences which justify that no general conclusions can be deduced from a priori equivalent ternary phase diagrams. A draft of the experimental pseudoternary Ni–(Ga,Al)–As diagram for the atomic Ga/Al ratio of 0.7/0.3 has been made which displays the same main features as those of the Ni–Al–As one.

On the basis of this work and as confirmed by studies done on thin film Ni/AlAs structures [12], NiAl has been found to be a good candidate for thermodynamically stable contacts to AlAs, since NiAl/AlAs and AlAs/NiAl/AlAs heterostructures and NiAl, AlAs superlattices have been realized [37–39].

Acknowledgement

This work was supported by the Centre National d'Etudes des Télécommunications, CNET Lannion B (FRANCE TELECOM) under contract 88 8B 073.

References

[1] R. Guérin, A. Guivarc'h, Y. Ballini and M. Secoué, *Rev. Phys. Appl., 25* (1990) 411.
[2] A. Guivarc'h, R. Guérin, J. Caulet, A. Poudoulec and J. Fontenille, *J. Appl. Phys., 66* (1989) 2129.
[3] S. Députier, A. Guivarc'h, J. Caulet, M. Minier and R. Guérin, *J. Phys. III, 4* (1994) 867.
[4] S. Députier, *Thèse d'Université,* Rennes, 1992.
[5] A. Guivarc'h, M. Secoué and B. Guenais, *J. Appl. Phys., 64* (1988) 683.
[6] A. Guivarc'h, M. Secoué and B. Guenais, *Appl. Phys. Lett., 52* (1988) 948.
[7] A. Guivarc'h, J. Caulet, B. Guenais, Y. Ballini, R. Guérin, A. Poudoulec and A. Regreny, *J. Cryst. Growth, 95* (1989) 427.
[8] A. Guivarc'h, R. Guérin and M. Secoué, *Electron. Lett., 23* (1987) 1004.
[9] A. Le Corre, B. Guenais, A. Guivarc'h, D. Lecrosnier, J. Caulet, M. Minier, G. Ropars, P.A. Badoz and J.-Y. Duboz, *J. Cryst. Growth, 105* (1990) 234.
[10] R. Guérin and A. Guivarc'h, *J. Appl. Phys., 66* (1989) 2122.
[11] S. Députier, R. Guérin, Y. Ballini and A. Guivarc'h, *J. Alloys Comp., 202* (1993) 95.
[12] S. Députier, A. Guivarc'h, J. Caulet, M. Minier, A. Poudoulec and R. Guérin, *J. Phys. III,* in press.
[13] T.B. Massalski, *Binary Alloy Phase Diagrams,* American Society for Metals, Metals Park, OH, 2nd edn., 1990.
[14] P. Villars and L.D. Calvert, *Pearson's Handbook of Crystallographic Data for Intermetallic Phases,* American Society for Metals, Metals Park, OH, 1991.
[15] R.A. Yund, *Econ. Geol., 56* (1961) 1273.
[16] A. Kjekshus and K.J. Skang, *Acta Chem. Scand., 27* (1973) 582.
[17] G. Aminoff, *Z. Kristallogr., 58* (1923) 203.
[18] A. Kjekshus and T. Rakke, *Acta Chem. Scand. A33* (1979) 609.
[19] A. Kjekshus, T. Rakke and A.F. Andresen, *Acta Chem. Scand. A, 28* (1974) 996.
[20] K. Aoki and O. Izumi, *Phys. Status Solidi A, 32* (1975) 657.
[21] F. Reynaud, *J. Appl. Crystallogr., 9* (1976) 263.
[22] I.M. Robertson and C.M. Wayman, *Metallography, 17* (1984) 43.
[23] M. Ellner, S. Kek and B. Predel, *J. Less-Common Met., 154* (1989) 207.
[24] A.J. Bradley and A. Taylor, *Philos. Mag., 23* (1937) 1049.
[25] L.M. Foster, J.E. Scardefield and J.F. Woods, *J. Electrochem. Soc., Solid State Sci. Technol., 119* (1972) 765.
[26] A. Taylor and N.J. Doyle, *J. Appl. Crystallogr., 5* (1972) 201.
[27] C.T. Tsai and R.S. Williams, *J. Mater Res., 1* (1986) 352.
[28] R. Beyers, K.B. Kim and R. Sinclair, *J. Appl. Phys., 61* (1987) 2195.
[29] L. Pauling, *Nature of the Chemical Bond,* Cornell University Press, Ithaca, NY, 3rd edn., 1960.
[30] F. Jellinek, *Oster. Chem. Z., 311* (1960) 81.
[31] E. Hellner, *Z. Metallk., 41* (1950) 480.
[32] A. Poudoulec, B. Guenais, A. Guivarc'h, J. Caulet and R. Guérin, *J. Appl. Phys., 70* (1991) 7613.
[33] A.R. Miedema, R. Boom and F.R. de Boer, *J. Less-Common Met., 41* (1975) 283.
[34] A.R. Miedema, *J. Less-Common Met., 46* (1976) 67.
[35] A.R. Miedema, P.F. de Châtel and F.R. de Boer, *Physica B, 100* (1980) 1.
[36] A.K. Niessen, F.R. de Boer, R. Boom, P.F. de Châtel, W.C.M. Mattens and A.R. Miedema, *Calphad, 7*(1) (1983) 51.
[37] J.P. Harbison, T. Sands, N. Tabatabaie, W.K. Chan, L.T. Florez and V.G. Keramidas, *Appl. Phys. Lett., 53* (1988) 1717.
[38] T. Sands, J.P. Harbison, N. Tabatabaie, W.K. Chan, H.L. Gilchrist, T.L. Cheeks, L.T. Florez and V.G. Keramidas, *Surf. Sci., 228* (1990) 1.
[39] C.J. Palmstrøm and T. Sands, in L.J. Brillson (ed.), *Contacts to Semiconductors,* Noyes, Park Bridge, NJ, (1993) 67.